Rakenteiden Mekaniikka (Journal of Structural Mechanics)
Vol. 47, No 2, 2014, pp. 50 – 66

A continuum damage model based on Ottosen's four parameter failure criterion for concrete

Saba Tahaei Yaghoubi, Reijo Kouhia[1], Juha Hartikainen and Kari Kolari

Summary. In this paper, a thermodynamic formulation for modelling anisotropic damage of elastic-brittle materials based on Ottosen's 4-parameter failure surface is proposed. The model is developed by using proper expressions for the specific Gibbs free energy and the complementary form of the dissipation potential. The formulation predicts the behaviour of the material relevantly and suggests a realistic shape for the damage surface.

Key words: damage, elastic-brittle material, constitutive equation, the specific Gibbs free energy, Helmholtz free energy, dissipation potential, Ottosen's 4-parameter criterion, damage surface

Received 6 June 2014. Accepted 28 August 2014. Published online 31 October 2014

Introduction

Non-linear behaviour of quasi-brittle materials such as concrete has been the topic of various investigations in the last decades. It is well-known that the non-linear behaviour of such materials under loading is mainly due to damage and micro-cracking rather than plastic deformation [15]. The generation of micro-cracks results in gradual loss of elasticity, volume dilatancy, strain-softening, etc [6]. Damage of concrete has been studied by several authors using a scalar damage variable which was first defined by Kachanov in 1958 [8], vector or higher order damage tensors. Scalar damage variables were utilized by authors such as Mazars and Pijaudier-Cabot [15] or Lee and Fenves [13]. Mikkola and Piila [16] described the response of concrete in uniaxial tension and compression by using damage vectors as internal variables. Second order damage tensors have been applied in order to model the anisotropic damage of rock-like materials by researchers such as Dragon *et al.* [6] or Murakami and Kamiya [18]. However, experimental investigations indicate that failure of rock-like materials in tension is mainly due to the growth of the most critical micro-crack while the compressive behaviour is much more complex and can be seen as a cooperative action of a distributed microcrack array [2]. Hence, application of a scalar damage parameter will not describe the behaviour of such materials properly.

In 1997, Murakami and Kamiya [18] modelled the anisotropic behaviour of elastic-brittle materials under multiaxial state of stress by using a second order damage tensor. They proposed a thermodynamically consistent formulation in which the specific Helmholtz free energy is described in terms of elastic strain and damage tensor and the damage dissipation potential is expressed in terms of damage conjugate force. Equivalent thermodynamic force is defined as a norm of the thermodynamic force conjugate to the

[1]Corresponding author. reijo.kouhia@tut.fi

damage rate and isotropic hardening is adopted to model the evolution of the damage surface. Furthermore, a modified elastic strain tensor is introduced in the strain energy function to adjust the shape of the damage dissipation potential. However, the shape of the damage surface does not describe the well-known properties of the brittle materials and consequently the ultimate fracture stress in uniaxial tension is approximately 25% of final uniaxial compressive stress. The modified elastic strain facilitates description of the brittle material to a great extent. However, the obtained results do not conform to the experimental observations in such materials since it is well-known that the uniaxial tensile strength of brittle materials such as concrete is $5-10\%$ of their uniaxial compressive strength and a proper description of the damage surface is critical in prediction of the behaviour of materials subjected to damage. Furthermore, the new term introduced in the strain energy makes the numerical calculation procedure complicated.

In the present study, a new continuum damage formulation which has the same features as Ottosen's 4-parameter criterion [20] is proposed. The elastic behavior of the material is captured by a specific Gibbs free energy function with stress and the second rank symmetric damage tensor as the state variables and internal variable κ which controls the size of the damage surface. The complementary dissipation potential is formulated using Ottosen's 4-parameter criterion in the damage conjugate force space. The new formulation predicts a proper shape for the damage surface which is similar to the shape obtained by Ottosen's model.

In the next two sections, constitutive models for concrete and Ottosen's 4-parameter criterion [20] will be reviewed briefly. Next, the new constitutive equations are derived. At the end, the technique applied for the solution of the system of equations is explained and some numerical results are presented.

Constitutive models for concrete

Concrete is a mixture of cement, water and aggregates in certain proportions. Aggregate fills about 80 % and the cement binder 12-14 % of the concrete volume. For normal strength concrete with compressive uniaxial strength in the range 20-60 MPa, the bond between the aggregate and the cement paste affects the strength of a concrete crucially [1].

One characteristic feature in mechanical behaviour of concrete is its low tensile strength. It results in cracking and highly anisotropic stress-strain behaviour. Classically concrete has been modelled as an elastic-plastic continuum, in which the cracks have been taken into account (i) as discrete cracks, (ii) in a smeared fashion or (iii) utilizing the continuum damage theories [10, 9, 16].

Classic failure models of concrete are the models by Willam-Warnke [23], Ottosen [20, 21, 22], Lubliner [14] and Lee [12, 13].

Ottosen 4-parameter failure criterion

Characteristic features for the failure surface of concrete are the following.

1. The uniaxial tensile strength is $5-10\%$ of the uniaxial compressive strength.
2. The shape of the failure curves on the meridian plane is slightly curved.
3. Hydrostatic compression cannot cause failure.
4. The shape of the failure locus on the deviatoric plane is triangular for small hydrostatic pressure and gets rounded with increasing hydrostatic pressure.

In 1977 Ottosen proposed a constitutive model for concrete which is one of the best models which can predict the above mentioned features with four material parameters only [20, 21, 22]. In this article, the Ottosen's damage surface has been reformulated based on the continuum damage theory.

The Ottosen's 4-parameter failure criterion has the form:

$$A\frac{J_2}{\sigma_c} + \Lambda\sqrt{J_2} + BI_1 - \sigma_c = 0, \tag{1}$$

where σ_c stands for the uniaxial compressive strength of the material, $I_1 = \mathrm{tr}\,\boldsymbol{\sigma}$ is the first invariant of the stress tensor and $J_2 = \frac{1}{2}\boldsymbol{s} : \boldsymbol{s}$ the second invariant of the deviatoric stress tensor $\boldsymbol{s} = \boldsymbol{\sigma} - \sigma_m\boldsymbol{I}$, where σ_m is the mean normal stress $\sigma_m = \frac{1}{3}I_1$. Furthermore, the shape of the failure surface is determined by the function $\Lambda = \Lambda(\theta)$, defined as

$$\Lambda = \begin{cases} k_1\cos[\frac{1}{3}\arccos(k_2\cos 3\theta)] & \text{if} \quad \cos 3\theta \geqslant 0 \\ k_1\cos[\frac{1}{3}\pi - \frac{1}{3}\arccos(-k_2\cos 3\theta)] & \text{if} \quad \cos 3\theta \leq 0 \end{cases}. \tag{2}$$

In equation (2), $\cos 3\theta$ is the Lode angle in the deviatoric plane defined in terms of the deviatoric invariants as

$$\cos 3\theta = \frac{3\sqrt{3}}{2}\frac{J_3}{J_2^{3/2}}, \tag{3}$$

where $J_3 = \det \boldsymbol{s}$ is the third invariant of the deviatoric stress tensor. In equations (1) and (2); A, B, the size factor k_1 and the shape factor k_2 are dimensionless material parameters with the limitations

$$A \geqslant 0; \quad B \geqslant 0; \quad k_1 \geqslant 0; \quad 0 \leq k_2 \leq 1. \tag{4}$$

Obviously, for $A = k_2 = 0$ the failure surface of equation (1) converts into Drucker-Prager criterion which can be reduced into von Mises criterion if $B = 0$. The shape of the failure surface is shown in Fig.1 in the meridian and deviatoric planes as well as under plane-stress condition and for a (σ, τ)-stress state.

The parameters A, B, k_1 and k_2 can be determined from the failure stress state of four tests:

1. uniaxial tensile test σ_t,
2. uniaxial compression test, failure stress σ_c,
3. equibiaxial compressive stress σ_{bc},
4. a failure stress state on the compressive meridian $(\sigma_{m4}, \sigma_{e4})$, where σ_e is the effective stress $\sigma_e = \sqrt{3J_2}$.

With these four tests values for the parameters A, B, k_1 and k_2 can be expressed in terms of $\sigma_c, \sigma_t, \sigma_{bc}$ and $(\sigma_{m4}, \sigma_{e4})$.

First, values of the Λ-parameter on the tensile- and compressive meridians are determined

$$\Lambda_t = \Lambda(0^\circ) = k_1\cos(\tfrac{1}{3}\arccos k_2), \tag{5}$$

$$\Lambda_c = \Lambda(60^\circ) = k_1\cos[\tfrac{1}{3}(\pi - \arccos k_2)]. \tag{6}$$

The failure states 3 and 1 which are on the tensile meridian, result in conditions

$$\tfrac{1}{3}(\bar{\sigma}_{bc})^2\,A + \tfrac{1}{\sqrt{3}}\bar{\sigma}_{bc}\,\Lambda_t - 2\bar{\sigma}_{bc}\,B - 1 = 0, \tag{7}$$

$$\tfrac{1}{3}(\bar{\sigma}_t)^2\,A + \tfrac{1}{\sqrt{3}}\bar{\sigma}_t\,\Lambda_t + \bar{\sigma}_t\,B - 1 = 0, \tag{8}$$

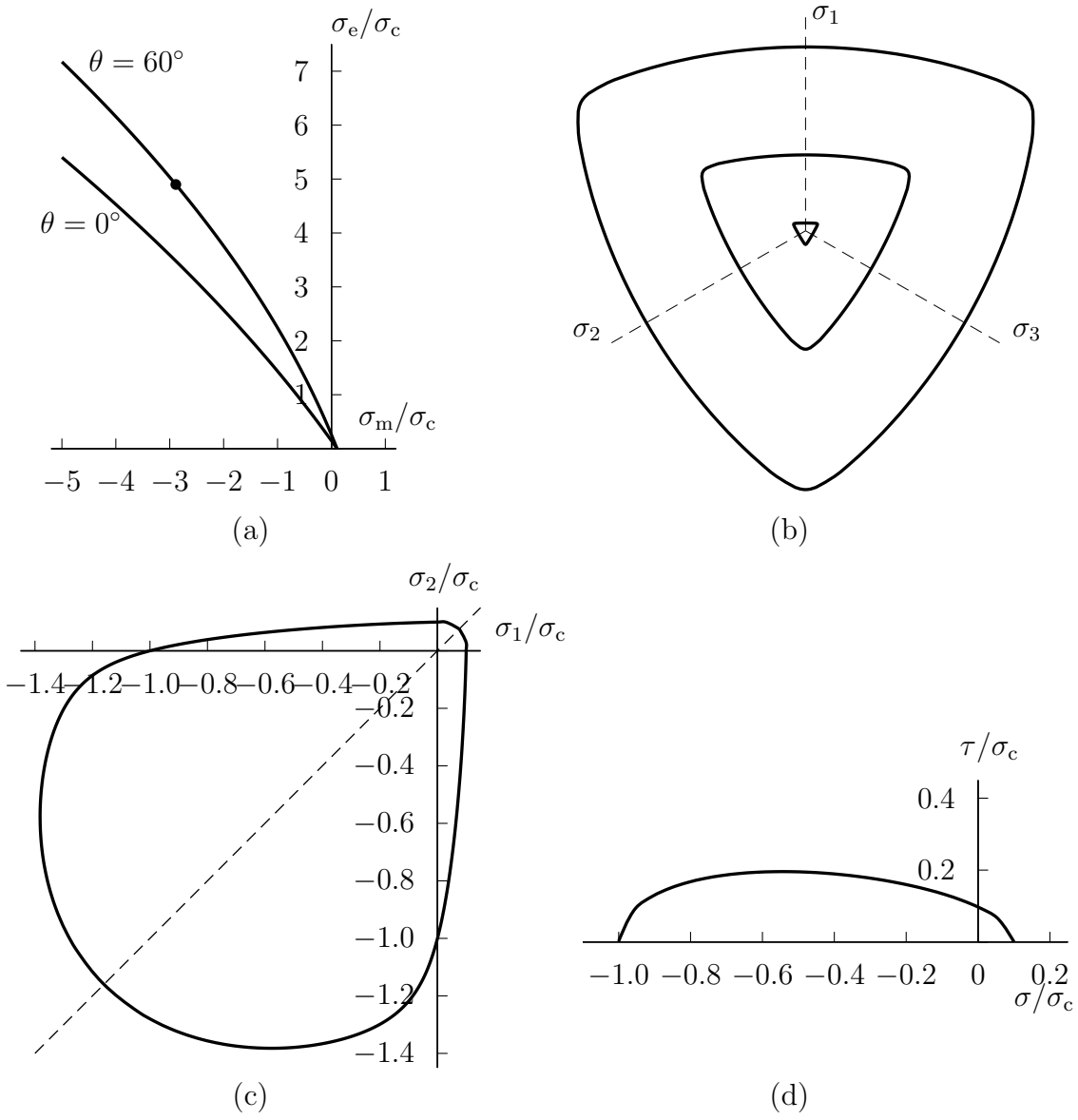

Figure 1. Ottosen's 4-parameter failure surface ($\sigma_c/\sigma_t = 10, \bar{\sigma}_{bc} = 1,16, \sigma_{m4} = -2.887\sigma_c, \sigma_{e4} = 4.899\sigma_c$): (a) meridian plane (b) deviatoric plane when $\sigma_m = 0$ (π-plane), $\sigma_m = -\sigma_c$ and $\sigma_m = -2,887\sigma_c$, (c) plane stress and (d) (σ, τ)-stress state.

where the dimensionless failure stress ratios $\bar{\sigma}_{\mathrm{bc}} = \sigma_{\mathrm{bc}}/\sigma_{\mathrm{c}}$ and $\bar{\sigma}_{\mathrm{t}} = \sigma_{\mathrm{t}}/\sigma_{\mathrm{c}}$ have been used.

Correspondingly, the failure stress states on the compressive meridian results in

$$\tfrac{1}{3}A + \tfrac{1}{\sqrt{3}}\Lambda_{\mathrm{c}} - B - 1 = 0, \tag{9}$$

$$\tfrac{1}{3}\bar{\sigma}_{\mathrm{e4}}^2\, A + \tfrac{1}{\sqrt{3}}\bar{\sigma}_{\mathrm{e4}}\,\Lambda_{\mathrm{c}} + 3\bar{\sigma}_{\mathrm{m4}}\, B - 1 = 0, \tag{10}$$

where the non-dimensional stresses $\bar{\sigma}_{\mathrm{m}}$ and $\bar{\sigma}_{\mathrm{e}}$ are

$$\bar{\sigma}_{\mathrm{m4}} = \frac{\sigma_{\mathrm{m4}}}{\sigma_{\mathrm{c}}}, \quad \bar{\sigma}_{\mathrm{e4}} = \frac{\sigma_{\mathrm{e4}}}{\sigma_{\mathrm{c}}}. \tag{11}$$

From equations (7) and (9) the unknowns Λ_{t} and Λ_{c} can be solved, and the result is

$$\Lambda_{\mathrm{t}} = \sqrt{3}[\frac{1}{\bar{\sigma}_{\mathrm{bc}}} + 2B - \frac{\bar{\sigma}_{\mathrm{bc}}}{3}A], \tag{12}$$

$$\Lambda_{\mathrm{c}} = \sqrt{3}[1 + B - \tfrac{1}{3}A]. \tag{13}$$

Substituting these expressions back to equations (8) and (10), a linear equation system for solution of the parameters A and B is obtained

$$\bar{\sigma}_{\mathrm{e4}}A + \frac{9\bar{\sigma}_{\mathrm{m4}} + 3\bar{\sigma}_{\mathrm{e4}}}{\bar{\sigma}_{\mathrm{e4}} - 1}\, B = -3, \tag{14}$$

$$A - \frac{9m}{m\bar{\sigma}_{\mathrm{bc}} - 1}\, B = -\frac{3m}{\bar{\sigma}_{\mathrm{bc}}}, \tag{15}$$

where $m = 1/\bar{\sigma}_{\mathrm{t}} = \sigma_{\mathrm{c}}/\sigma_{\mathrm{t}}$. Thus the coefficients A and B are completely determined from the strengths $\sigma_{\mathrm{t}}, \sigma_{\mathrm{c}}, \sigma_{\mathrm{bc}}$, and from the point on the compressive meridian $(\sigma_{\mathrm{m4}}, \sigma_{\mathrm{e4}})$, and the solution is

$$B = \frac{m\bar{\sigma}_{\mathrm{e4}}/\bar{\sigma}_{\mathrm{bc}} - 1}{\xi + \dfrac{3m\bar{\sigma}_{\mathrm{e4}}}{m\bar{\sigma}_{\mathrm{bc}} - 1}}, \tag{16}$$

$$A = \frac{9m}{m\bar{\sigma}_{\mathrm{bc}} - 1}\, B - \frac{3m}{\bar{\sigma}_{\mathrm{bc}}}, \tag{17}$$

where the ξ is defined as

$$\xi = \frac{3\bar{\sigma}_{\mathrm{m4}} + \bar{\sigma}_{\mathrm{e4}}}{\bar{\sigma}_{\mathrm{e4}} - 1}. \tag{18}$$

Now the values for Λ can be determined from expressions (12) and (13). Denoting

$$\alpha = \tfrac{1}{3}\arccos k_2, \tag{19}$$

and using the identity $\cos(\pi/3 - \alpha) = \cos(\pi/3)\cos\alpha + \sin(\pi/3)\sin\alpha$ the following equations are obtained

$$\Lambda_{\mathrm{t}} = k_1 \cos\alpha, \tag{20}$$

$$\begin{aligned}\Lambda_{\mathrm{c}} &= \tfrac{1}{2}k_1(\cos\alpha + \sqrt{3}\sin\alpha) \\ &= \tfrac{1}{2}(\Lambda_{\mathrm{t}} + \sqrt{3}\sqrt{k_1^2 - \Lambda_{\mathrm{t}}^2}).\end{aligned} \tag{21}$$

Table 1. Parameter values and their dependence on the σ_t/σ_c-ratio.

σ_t/σ_c	A	B	k_1	k_2
0.08	1.8076	4.0962	14.4863	0.9914
0.10	1.2759	3.1962	11.7365	0.9801
0.12	0.9218	2.5969	9.9110	0.9647

Solution for k_1 and k_2 is

$$k_1 = \frac{2}{\sqrt{3}}\sqrt{\Lambda_t^2 + \Lambda_c^2 - \Lambda_t\Lambda_c}, \tag{22}$$

$$k_2 = \cos 3\alpha = 4\cos^3\alpha - 3\cos\alpha \tag{23}$$

$$= \left(\frac{\Lambda_t}{k_1}\right)\left[4\left(\frac{\Lambda_t}{k_1}\right)^2 - 3\right]. \tag{24}$$

Using the test results of Kupfer *et al.* [11], i.e. the equibiaxial compressive stress is $\sigma_{bc} = 1.16\sigma_c$ and the point on the compressive meridian as ($\sigma_{m4} = -2.887\sigma_c, \sigma_{e4} = 4.899\sigma_c$). The parameter values with different ratios of σ_t/σ_c are given in table 1, where σ_t denotes the uniaxial tensile strength of the material. Furthermore, the shape of the failure surface with different ratios of σ_t/σ_c is shown in Fig.2 in π-plane and plane stress condition. In practice, often only the compressive failure stress is known. Based on extensive experimental testing Dahl [5] proposed the following approximations for the parameters A, B, k_1 and k_2 based solely on the uniaxial compressive stress σ_c:

$$x = \sigma_c/\sigma_{c,ref}, \qquad \sigma_{c,ref} = 100\,\text{MPa}, \tag{25}$$

$$A = -1,66\,x^2 + 3,49\,x + 0,73, \tag{26}$$

$$B = -0,19\,x^2 + 0,41\,x + 3,13, \tag{27}$$

$$k_1 = \;\; 0,46\,x^2 - 0,97\,x + 11,89, \tag{28}$$

$$k_2 = -0,02\,x^2 + 0,04\,x + 0,974. \tag{29}$$

These expressions are fitted from data for normal and high-strength concrete ($\sigma_c < 80$ MPa). In deriving these expressions Dahl assumed that the equibiaxial compressive stress is $\sigma_{bc} = 1.16\sigma_c$ and that the uniaxial tensile strength is one-tenth of the uniaxial compressive strength.

Thermodynamic formulation

In this paper it has been assumed that deformations are fully elastic. The constitutive equations for a elastic-damaging solid are derived by using dissipation potentials and the mechanical part of the specific Gibbs free energy. Elastic behaviour is captured by the mechanical part of the specific Gibbs free energy function

$$\psi^c = \psi^c(S), \tag{30}$$

which is defined by the state variables $S = (\boldsymbol{\sigma}, \boldsymbol{D}, \kappa)$, where $\boldsymbol{\sigma}$ is the stress tensor, $\boldsymbol{D}$ the second order damage tensor and κ a set of internal variables characterizing the state

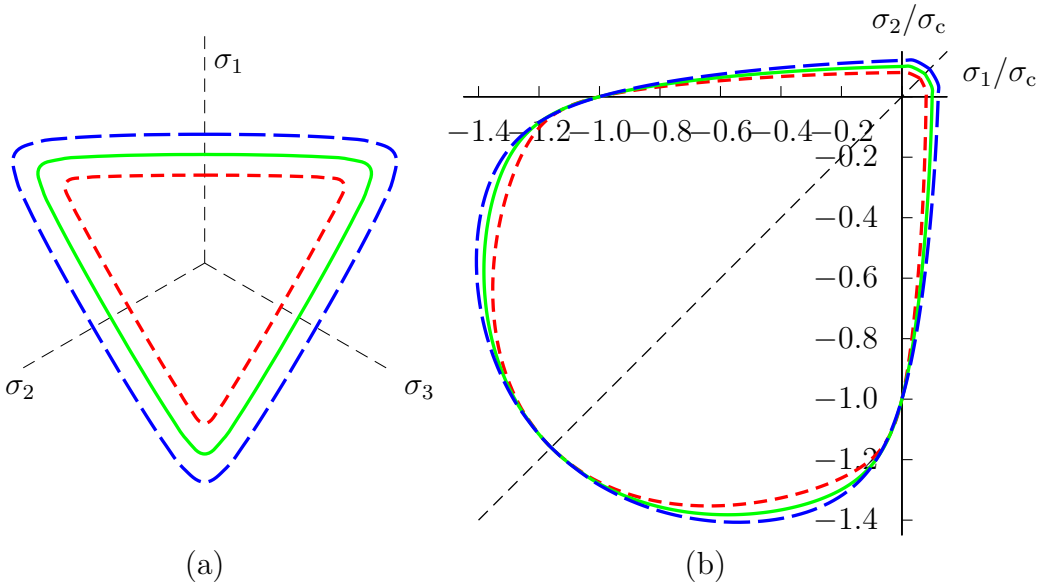

Figure 2. Ottosen's 4-parameter failure surface ($\sigma_{bc} = 1.16\sigma_c$), effect of the variation of the tensile strength: (a) π-plane (b) plane-stress. The point on the compressive meridian $\sigma_m = -\sigma_c$ and $\sigma_m = -2,887\sigma_c$. Red dashed line corresponds to $\sigma_t/\sigma_c = 0.08$, green solid line $\sigma_t/\sigma_c = 0.1$ and blue (long) dashed line $\sigma_t/\sigma_c = 0.12$.

of the material [22]. In general, the internal variables can be scalars or tensors. The specific Gibbs and Helmholtz free energies are related together by the partial Legendre transformation such that

$$\rho_0\psi(\boldsymbol{\varepsilon}, \boldsymbol{D}, \kappa) + \rho_0\psi^c(\boldsymbol{\sigma}, \boldsymbol{D}, \kappa) = \boldsymbol{\sigma} : \boldsymbol{\varepsilon}, \tag{31}$$

where ρ_0 stands for the material density and $\boldsymbol{\varepsilon}$ denotes the infinitesimal elastic strain tensor.

A thermodynamically admissible formulation satisfies the mechanical part of the Clausius-Duhem inequality which in isothermal case and without any heat supply takes the form

$$\gamma = -\rho_0\dot{\psi} + \dot{\boldsymbol{\varepsilon}} : \boldsymbol{\sigma}, \quad \gamma \geqslant 0. \tag{32}$$

where γ is the power of dissipation. Using equation (31) the power of dissipation can be reformulated as

$$\gamma = \rho_0\dot{\psi}^c - \dot{\boldsymbol{\sigma}} : \boldsymbol{\varepsilon}. \tag{33}$$

The irreversible material behaviour is described through the dissipation potential

$$\varphi = \varphi(W; S) \tag{34}$$

which is a function of the dissipation variables $W = (\boldsymbol{Y}, K)$, where $\boldsymbol{Y}$ and K are the thermodynamic forces dual to the rates $\dot{\boldsymbol{D}}$ and $\dot{\kappa}$, respectively. The dissipation potential is a convex and subdifferentiable function from a linear space into $\bar{\mathbb{R}} = \mathbb{R} \cup \{+\infty\}$ and determines the power of dissipation such that

$$\gamma \equiv \boldsymbol{B}_Y : \boldsymbol{Y} + B_K K, \quad (\boldsymbol{B}_Y, B_K) \in \partial\varphi(W; S), \tag{35}$$

where $\boldsymbol{B}_Y$ and B_K are the components of the subgradient of $\varphi(W; S)$ and $\partial\varphi(W; S)$ is the subdifferential set of all subgradients [7]. The dissipation potential is capable of describing non-smooth material behaviour through constraints on the dissipation variables.

Combining definition of γ in equations (33) and (35) results in equation

$$\left(\rho_0 \frac{\partial \psi^{\mathrm{c}}}{\partial \boldsymbol{\sigma}} - \boldsymbol{\varepsilon}\right) : \dot{\boldsymbol{\sigma}} + \rho_0 \frac{\partial \psi^{\mathrm{c}}}{\partial \boldsymbol{D}} : \dot{\boldsymbol{D}} + \rho_0 \frac{\partial \psi^{\mathrm{c}}}{\partial \kappa} : \dot{\kappa} = \boldsymbol{B}_Y : \boldsymbol{Y} + B_K K \tag{36}$$

By defining

$$\boldsymbol{Y} = \rho_0 \frac{\partial \psi^{\mathrm{c}}}{\partial \boldsymbol{D}} \quad \text{and} \quad K = -\rho_0 \frac{\partial \psi^{\mathrm{c}}}{\partial \kappa}, \tag{37}$$

equation (36) results in

$$\left(\rho_0 \frac{\partial \psi^{\mathrm{c}}}{\partial \boldsymbol{\sigma}} - \boldsymbol{\varepsilon}\right) : \dot{\boldsymbol{\sigma}} + \left(\dot{\boldsymbol{D}} - \boldsymbol{B}_Y\right) : \boldsymbol{Y} + \left(-\dot{\kappa} - B_K\right) K = 0. \tag{38}$$

If the bracketed coefficients in equation (38) tend to zero, the equation holds for arbitrary $\dot{\boldsymbol{\sigma}}$, $\boldsymbol{Y}$ and K, and the following constitutive equations are obtained.

$$\boldsymbol{\varepsilon} = \rho_0 \frac{\partial \psi^{\mathrm{c}}}{\partial \boldsymbol{\sigma}}, \qquad \dot{\boldsymbol{D}} = \boldsymbol{B}_Y, \qquad \dot{\kappa} = -B_K. \tag{39}$$

It has been proved that this approach guarantees the fulfilment of the dissipation inequality if the dissipation potential is (i) convex and subdifferentiable, (ii) non-negative and (iii) is zero when there is no evolution of the dissipative quantities [7, Theorem 4.3].

Specific model

Using only a single scalar internal variable κ, a particular expression for the specific Gibbs free energy, describing the elastic material behaviour with the reduction effect due to damage, is given by

$$\rho_0 \psi^{\mathrm{c}}(\boldsymbol{\sigma}, \boldsymbol{D}, \kappa) = \frac{1+\nu}{2E} \mathrm{tr}\boldsymbol{\sigma}^2 - \frac{\nu}{2E}(1 + \alpha_1 \mathrm{tr}\boldsymbol{D})(\mathrm{tr}\boldsymbol{\sigma})^2 + \frac{\alpha_2}{E}\mathrm{tr}(\boldsymbol{\sigma}^2 \boldsymbol{D}) + H_0 \left(\frac{\kappa}{\kappa_0}\right)^2 \left(\frac{\kappa}{3\kappa_0} - \frac{1}{2}\right) \tag{40}$$

where ν denotes the Poisson's ratio, E stands for the elastic modulus and α_1, α_2, H_0 and κ_0 are newly introduced material parameters.

For determining the dissipation potential, the key issue is to define the elastic domain, i.e. the domain of admissible stresses inside the damage surface ($f = 0$), as a convex set of the thermodynamic force $\boldsymbol{Y}$ and the hardening variable K such that

$$\Sigma = \{(\boldsymbol{Y}, K) | f(\boldsymbol{Y}, K; \boldsymbol{\sigma}) \leqslant 0\}. \tag{41}$$

The damage surface is defined by reformulating the Ottosen's 4-parameter failure surface in terms of the thermodynamic force $\boldsymbol{Y}$, hardening variable K, and stress $\boldsymbol{\sigma}$ as

$$f(\boldsymbol{Y}, K; \boldsymbol{\sigma}) = \frac{A\tilde{J}_2}{\sigma_{\mathrm{c}0}} + \Lambda\sqrt{\tilde{J}_2} + BI_1 - (\sigma_{\mathrm{c}0} + K) = 0, \tag{42}$$

where the redefined deviatoric invariants have expressions

$$\tilde{J}_2 = \frac{1}{2}\left[\frac{E}{\alpha_2}\mathrm{tr}\,\boldsymbol{Y} + (\mathrm{tr}\boldsymbol{\sigma})^2\left(\frac{3\alpha_1\nu}{2\alpha_2} - \frac{1}{3}\right)\right], \tag{43}$$

$$\tilde{J}_3 = \frac{1}{3}\left[\frac{E}{\alpha_2}(\mathrm{tr}(\boldsymbol{\sigma}\,\boldsymbol{Y}) - \mathrm{tr}\boldsymbol{\sigma}\mathrm{tr}\,\boldsymbol{Y}) + \left(\frac{2}{9} - \frac{\alpha_1\nu}{\alpha_2}\right)(\mathrm{tr}\boldsymbol{\sigma})^3\right]. \tag{44}$$

Moreover, the Lode angle has the form

$$\cos 3\theta = \frac{3\sqrt{3}}{2}\frac{\tilde{J}_3}{\tilde{J}_2^{3/2}}. \tag{45}$$

In the expression of the damage surface (42), σ_{c0} denotes the initial elastic limit in uniaxial compression. The dissipation potential is then defined as

$$\varphi(\boldsymbol{Y}, K; \boldsymbol{\sigma}) = \mathrm{I}_\Sigma(\boldsymbol{Y}, K; \boldsymbol{\sigma}), \tag{46}$$

where $\mathrm{I}_\Sigma(\boldsymbol{Y}, K; \boldsymbol{\sigma})$ is the indicator function defined by [7]

$$\mathrm{I}_\Sigma(\boldsymbol{Y}, K; \boldsymbol{\sigma}) = \begin{cases} 0 & \text{if } (\boldsymbol{Y}, K) \in \Sigma \\ +\infty & \text{if } (\boldsymbol{Y}, K) \notin \Sigma \end{cases}. \tag{47}$$

The subdifferential of φ is defined by the set

$$\partial\varphi(\boldsymbol{Y}, K; \boldsymbol{\sigma}) = \begin{cases} \{(\boldsymbol{B}_Y, B_K)\}, & \text{if } (\boldsymbol{Y}, K) \in \Sigma, \\ \emptyset, & \text{if } (\boldsymbol{Y}, K) \notin \Sigma, \end{cases} \tag{48}$$

where the components $\boldsymbol{B}_Y$ and B_K of the subgradient are zero in the interior of the damage surface and equal to the components of the normal of the damage surface at point $(\boldsymbol{Y}, K)$ on the damage surface such that

$$(\boldsymbol{B}_Y, B_K) = \begin{cases} (\boldsymbol{0}, 0), & \text{if } f(\boldsymbol{Y}, K_\alpha; \boldsymbol{\sigma}) < 0, \\ \left(\dot{\lambda}\dfrac{\partial f}{\partial \boldsymbol{Y}}, \dot{\lambda}\dfrac{\partial f}{\partial K}\right),\ \dot{\lambda} \geq 0, & \text{if } f(\boldsymbol{Y}, K_\alpha; \boldsymbol{\sigma}) = 0, \end{cases} \tag{49}$$

Above, $\dot{\lambda}$ is a multiplier that can be calculated by use of the consistency condition $\dot{f} = 0$.

Using equations (37), (39) and (49) the following constitutive equations are obtained:

$$\boldsymbol{\varepsilon} = \rho_0\frac{\partial \psi^{\mathrm{c}}}{\partial \boldsymbol{\sigma}} = \frac{1+\nu}{E}\boldsymbol{\sigma} - \frac{\nu}{E}(1 + \alpha_1 \mathrm{tr}\boldsymbol{D})(\mathrm{tr}\boldsymbol{\sigma})\boldsymbol{I} + \frac{\alpha_2}{E}(\boldsymbol{\sigma}\boldsymbol{D} + \boldsymbol{D}\boldsymbol{\sigma}), \tag{50}$$

$$\boldsymbol{Y} = \rho_0\frac{\partial \psi^{\mathrm{c}}}{\partial \boldsymbol{D}} = -\frac{\alpha_1\nu}{2E}(\mathrm{tr}\boldsymbol{\sigma})^2\boldsymbol{I} + \frac{\alpha_2}{E}\boldsymbol{\sigma}^2, \tag{51}$$

$$\dot{\boldsymbol{D}} = \dot{\lambda}\frac{\partial f}{\partial \boldsymbol{Y}} = \dot{\lambda}\left[\frac{A}{\sigma_{c0}}\frac{\partial \tilde{J}_2}{\partial \boldsymbol{Y}} + \sqrt{\tilde{J}_2}\left(\frac{\partial \Lambda}{\partial \tilde{J}_2}\frac{\partial \tilde{J}_2}{\partial \boldsymbol{Y}} + \frac{\partial \Lambda}{\partial \tilde{J}_3}\frac{\partial \tilde{J}_3}{\partial \boldsymbol{Y}}\right) + \tfrac{1}{2}\frac{\partial \tilde{J}_2}{\partial \boldsymbol{Y}}\tilde{J}_2{}^{-1/2}\Lambda\right], \tag{52}$$

$$K = -\rho_0\frac{\partial \psi^{\mathrm{c}}}{\partial \kappa} = \frac{H_0\kappa}{\kappa_0^2}\left(1 - \frac{\kappa}{\kappa_0}\right), \tag{53}$$

$$\dot{\kappa} = -\dot{\lambda}\frac{\partial f}{\partial K} = \dot{\lambda}. \tag{54}$$

Algorithmic treatment

In order to solve the constitutive equations, implicit Euler method together with Newton-Raphson iterative technique has been applied. The solution algorithm is summarized as follows.

1. Increase the strain value by the increment $\Delta\boldsymbol{\varepsilon}$ and compute the trial elastic stress.

$$\boldsymbol{\varepsilon}_{n+1} = \boldsymbol{\varepsilon}_n + \Delta\boldsymbol{\varepsilon} \tag{55}$$

$$\boldsymbol{\sigma}^{\text{trial}}_{n+1} = \frac{E}{1+\nu}\left(\boldsymbol{\varepsilon}_{n+1} + \frac{\nu\,\text{tr}(\boldsymbol{\varepsilon}_{n+1})}{1-2\nu}\boldsymbol{I}\right) \tag{56}$$

$$\boldsymbol{Y}^{\text{trial}}_{n+1} = -\frac{\alpha_1\nu}{2E}(\text{tr}\,\boldsymbol{\sigma}^{\text{trial}}_{n+1})^2\boldsymbol{I} + \frac{\alpha_2}{E}(\boldsymbol{\sigma}^{\text{trial}}_{n+1})^2 \tag{57}$$

where the subscripts correspond to the step numbers.

2. Check the damage condition

$$f^{\text{trial}}_{n+1} = \frac{A\tilde{J}_2}{\sigma_{\text{c0}}} + \Lambda\sqrt{\tilde{J}_2} + BI_1 - (\sigma_{\text{c0}} + K), \tag{58}$$

where $\tilde{J}_2 = \tilde{J}_2(\boldsymbol{Y}^{\text{trial}}_{n+1}, \boldsymbol{\sigma}^{\text{trial}}_{n+1})$ and $I_1 = I_1(\boldsymbol{\sigma}^{\text{trial}}_{n+1})$.

IF $f^{\text{trial}}_{n+1} \leq 0$ THEN:
Set

$$\boldsymbol{\varepsilon}_{n+1} = \boldsymbol{\varepsilon}_n \tag{59}$$

$$\boldsymbol{\sigma}_{n+1} = \boldsymbol{\sigma}^{\text{trial}}_{n+1} \tag{60}$$

$$\boldsymbol{Y}_{n+1} = \boldsymbol{Y}^{\text{trial}}_{n+1} \tag{61}$$

& NEXT STEP.
ENDIF.

3. Solve $f(\lambda_{n+1}) = 0$. [2]
Use Newton-Raphson iterative method.

- Compute the iterative change $\delta\lambda$

$$f(\lambda^i_{n+1}) + f'(\lambda^i_{n+1})\delta\lambda = 0. \tag{63}$$

$$f(\lambda^i_{n+1}) = f(\boldsymbol{Y}^i_{n+1}, K^i_{n+1}; \boldsymbol{\sigma}^i_{n+1}). \tag{64}$$

$$\delta\lambda = \lambda^{i+1}_{n+1} - \lambda^i_{n+1} \tag{65}$$

  where the superscripts refer to iteration number.

- Update $\boldsymbol{D}$

$$\boldsymbol{D}^{i+1}_{n+1} = \boldsymbol{D}^i_{n+1} + \delta\lambda\frac{\partial f^i_{n+1}}{\partial \boldsymbol{Y}^i_{n+1}} \tag{66}$$

- Update K

$$\kappa^{i+1}_{n+1} = \kappa^i_{n+1} + \delta\lambda \tag{67}$$

$$K^{i+1}_{n+1} = \frac{H_0\kappa^{i+1}_{n+1}}{\kappa_0^2}(1 - \frac{\kappa^{i+1}_{n+1}}{\kappa_0}) \tag{68}$$

[2] $f(\lambda)$ is calculated using equation (42) and $f'(\lambda)$ can be obtained based on chain rule as

$$f'(\lambda) = \frac{\partial f}{\partial \boldsymbol{Y}} : \frac{\partial \boldsymbol{Y}}{\partial\lambda} + \frac{\partial f}{\partial \boldsymbol{\sigma}} : \frac{\partial \boldsymbol{\sigma}}{\partial\lambda} + \frac{\partial f}{\partial K}\frac{\partial K}{\partial\lambda}. \tag{62}$$

Since the equations are lengthy but readily obtained, they are not written in details in this article.

- Update $\boldsymbol{\sigma}$

$$\boldsymbol{\sigma}_{n+1}^{i+1} = \boldsymbol{C}_{n+1}^{i+1}\boldsymbol{\varepsilon}_{n+1} \tag{69}$$

The elasticity tensor $\boldsymbol{C}$ is the inverse of the compliance tensor $\boldsymbol{L}$

$$\boldsymbol{L} = \begin{bmatrix} L_{11} & -\eta_2 & -\eta_2 & 2\eta_3 D_{12} & 2\eta_3 D_{13} & 0 \\ -\eta_2 & L_{22} & -\eta_2 & 2\eta_3 D_{12} & 0 & 2\eta_3 D_{23} \\ -\eta_2 & -\eta_2 & L_{33} & 0 & 2\eta_3 D_{13} & 2\eta_3 D_{23} \\ \eta_3 D_{12} & \eta_3 D_{12} & 0 & L_{44} & \eta_3 D_{23} & \eta_3 D_{13} \\ \eta_3 D_{13} & 0 & \eta_3 D_{13} & \eta_3 D_{23} & L_{55} & \eta_3 D_{12} \\ 0 & \eta_3 D_{23} & \eta_3 D_{23} & \eta_3 D_{13} & \eta_3 D_{12} & L_{66} \end{bmatrix}, \tag{70}$$

where

$$\eta_1 = \frac{1+\nu}{E}, \qquad \eta_2 = \frac{\nu(1+\alpha_1 \operatorname{tr} \boldsymbol{D})}{E}, \qquad \eta_3 = \frac{\alpha_2}{E}, \tag{71}$$

and

$$L_{11} = \eta_1 - \eta_2 + 2\eta_3 D_{11}, \quad L_{22} = \eta_1 - \eta_2 + 2\eta_3 D_{22}, \quad L_{33} = \eta_1 - \eta_2 + 2\eta_3 D_{33}, \tag{72}$$

$$L_{44} = \eta_1 + \eta_3(D_{11} + D_{22}), \quad L_{55} = \eta_1 + \eta_3(D_{11} + D_{33}), \quad L_{66} = \eta_1 + \eta_3(D_{22} + D_{33}). \tag{73}$$

Numerical results

Uniaxial compression

The constitutive equations of (50)-(54) are solved for a concrete specimen with the ultimate compressive strength $\sigma_{\mathrm{c}} = 32.8$ MPa under uniaxial tension, uniaxial compression and biaxial compression. The initial values for the material parameters E and ν are obtained from the literature [3] as:

$$E = 32\,\mathrm{GPa}, \quad \nu = 0.2. \tag{74}$$

The values below for the material constants A, B, k_1 and k_2 are obtained by means of Ottosen's 4-parameter criterion and setting $\sigma_{\mathrm{c0}} = 18$ MPa and $\sigma_{\mathrm{t0}} = 1$ MPa where σ_{t0} is the initial elastic limit in uniaxial tension.

$$A = 2.9782, \quad B = 6.0781, \quad k_1 = 20.5560, \quad k_2 = 0.9990. \tag{75}$$

The values below for the remaining parameters are determined by using experimental results of uniaxial compression found in literature [11]

$$\alpha_1 = 5.2, \quad \alpha_2 = 10, \quad H_0 = 1353.36\,\mathrm{Pa}, \quad \kappa_0 = 8.15 \times 10^{-6}. \tag{76}$$

The predicted stress-strain curve for the concrete specimen under uniaxial compression is illustrated in Fig.3a. In Fig.3a $\varepsilon_{\mathrm{c}} = 0.212$ % denotes the value of strain when stress reaches the maximum compressive stress σ_{c}. As observed in the figure, the constitutive equations (50)-(54) together with the material parameters of equations (74)-(76) predict the behaviour of the material with acceptable accuracy in comparison with experimental observations [11].

In Fig.3b, damage-strain curves for the concrete specimen under uniaxial compression are illustrated. According to the figure, damage perpendicular to the loading $D_{22} =$

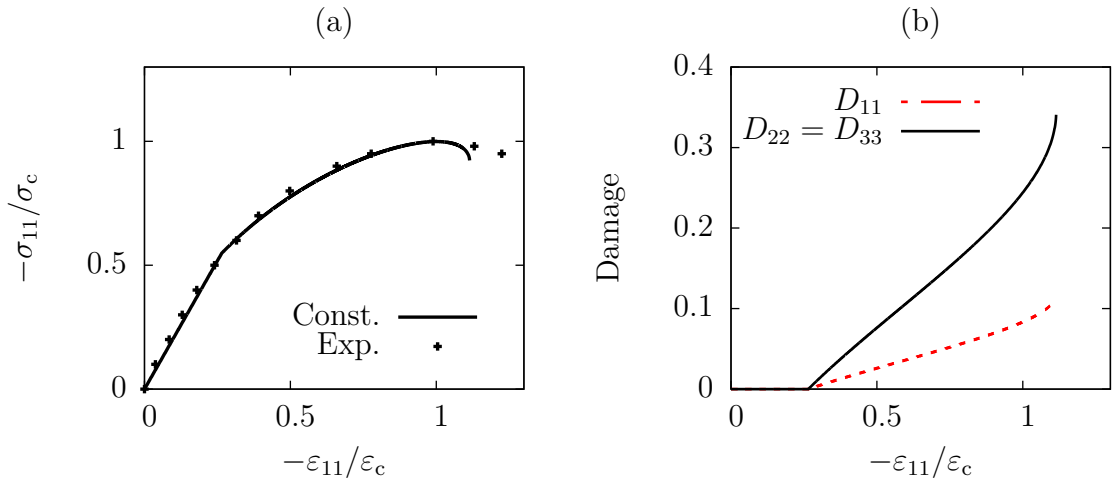

Figure 3. (a) Predicted stress-strain curve of the constitutive model for concrete specimen under uniaxial compression compared to experimental results [11], (b) Predicted damage-strain curves of the constitutive model for the concrete specimen under uniaxial compression.

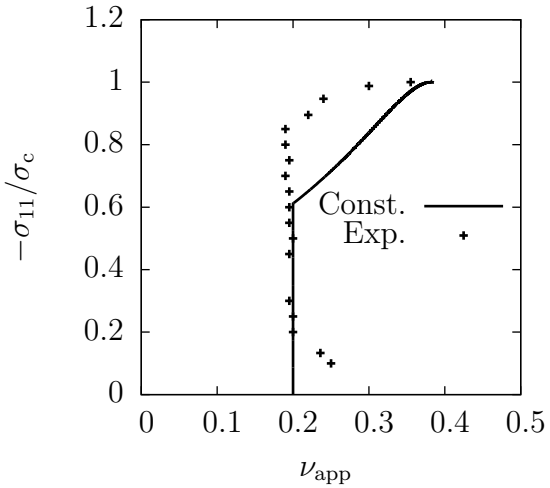

Figure 4. Apparent Poisson's ratio $\nu_{app} = -\varepsilon_{22}/\varepsilon_{11}$ of the concrete specimen under uniaxial compression plotted using the constitutive model compared to experimental results [4].

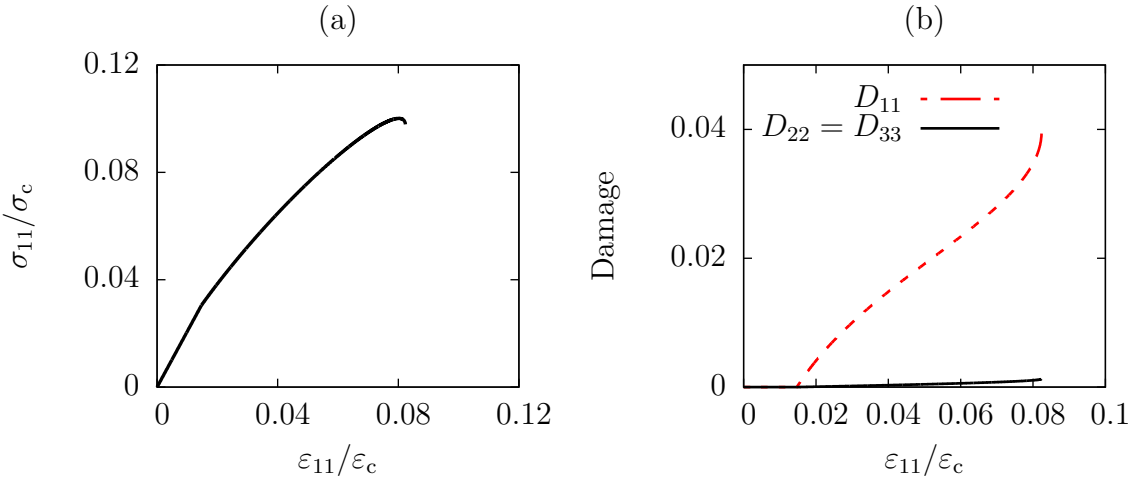

Figure 5. (a) Predicted stress-strain curve of the constitutive model for concrete specimen under uniaxial tension, (b) Predicted damage-strain curves of the constitutive model for the concrete specimen under uniaxial tension.

D_{33} is larger than damage parallel to the loading direction D_{11}. This is consistent with experimental observations for elastic-brittle materials [2, 18, 19].

Fig.4 shows the prediction of apparent Poisson's ratio-stress relation. The result is compared to the available data obtained form literature [4]. Apparent Poisson's ratio ν_{app} is continuously increasing after the compressive stress reaches the initial compressive strength $\sigma_{c0} = 18$ MPa.

Uniaxial tension

The stress-strain curve for the concrete specimen under uniaxial tension predicted by the constitutive equations (50)-(54) and the material parameters of equations (74)-(76) is shown in Fig.5a. According to the figure, the ratio between the maximum tensile and compressive strengths is $\sigma_t/\sigma_c = 0.1$ which is characteristic of elastic-brittle materials such as concrete [17].

Fig.5b shows the predicted damage-strain curves for the material under uniaxial tension. Damage parallel to the loading direction D_{11} is considerably larger than damage perpendicular to the loading $D_{22} = D_{33}$. Furthermore, a comparison between Fig.3b and Fig.5b shows that the difference between the values of the damage tensor is larger in tension than in compression. This is also in line with the nature of the elastic-brittle material, since the failure of such materials in compression is due to the cracks which are produced in directions both parallel and perpendicular to the loading direction, while growth of cracks in the perpendicular direction to the loading direction is mainly responsible for the failure of the material in tension [2, 18, 19].

Equibiaxial compression

Fig.6a shows the modelled behaviour of the concrete specimen under equibiaxial compression. Compared to the experimental observations, the model predicts a brittler behaviour for the material and the magnitude of strain ε_{11} corresponding to the ultimate stress is approximately 60% smaller than the results found in the literature [11]. This problem can be seen in the results of damage shown in Fig.6b. The damage parallel to the loading direction $D_{11} = D_{22}$ is unrealistically large compared to damage perpendicular to the

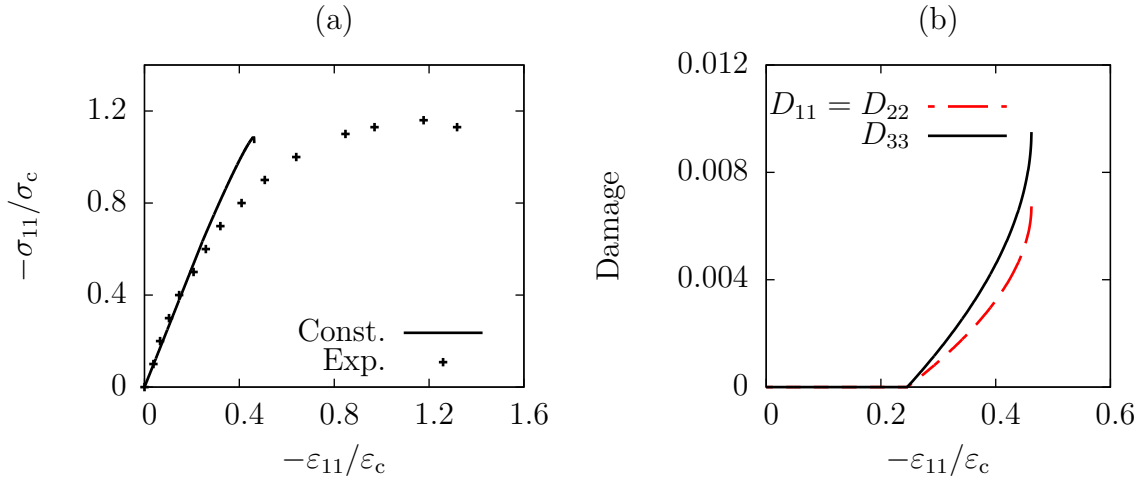

Figure 6. (a) Predicted stress-strain curve of the constitutive model for concrete specimen under equibiaxial compression compared to experimental results [11], (b) Predicted damage-strain curves of the constitutive model for the concrete specimen under equibiaxial compression.

loading D_{33}. Thus, although the model predicts the behaviour of the material in simple loading cases, the results are not in agreement with the experimental observations when the material is subjected to equibiaxial compressive stress.

Concluding remarks and future work

In this study, the 4-parameter Ottosen's failure model is reformulated in a damage conjugate force space and a thermodynamically consistent formulation for modelling the anisotropic damage of concrete is derived. The constitutive equations are obtained by choosing a proper expression for the specific Gibbs free energy and the dissipation potential which is a reformulation of the Ottosen's failure criterion. Using the second order damage tensor as a state variable makes it possible to predict the anisotropic behaviour of damage for elastic-brittle materials in simple loading cases. However, the results show some shortcomings when more general loading cases are considered. For example, the model does not predict the behavior of the material under biaxial compression properly. On the other hand, the approach can be easily extended to more advanced damage models. Therefore further investigations will be directed to develop a more advanced damage model which can predict the behaviour of material more realistically.

Appendix. Derivation of the invariant expressions $\tilde{J}_2$ and $\tilde{J}_3$

The second and third invariants of the deviatoric stress tensor have expressions

$$J_2 = \tfrac{1}{2}\boldsymbol{s} : \boldsymbol{s} = \tfrac{1}{2}\operatorname{tr}(\boldsymbol{s}^2), \tag{77}$$

$$J_3 = \det \boldsymbol{s} = \tfrac{1}{3}\operatorname{tr}(\boldsymbol{s}^3), \tag{78}$$

where $\boldsymbol{s}$ is the deviatoric stress tensor $\boldsymbol{s} = \boldsymbol{\sigma} - \frac{1}{3}I_1\boldsymbol{I}$ and $I_1 = \operatorname{tr}\boldsymbol{\sigma}$. Therefore the quadratic invariant of the deviatoric tensor can be expressed using the invarians of the tensor itself as

$$\operatorname{tr}(\boldsymbol{s}^2) = \operatorname{tr}(\boldsymbol{\sigma}^2) - \tfrac{1}{3}(\operatorname{tr}\boldsymbol{\sigma})^2. \tag{79}$$

From equation (51) one obtains

$$\mathrm{tr}(\boldsymbol{\sigma}^2) = \frac{E}{\alpha_2}\,\mathrm{tr}(\,\boldsymbol{Y}) + \frac{3\alpha_1\nu}{2\alpha_2}(\mathrm{tr}\,\boldsymbol{\sigma})^2. \tag{80}$$

Substituting equation (80) into equation (79) and using equation (77) results in

$$\tilde{J}_2 = \frac{1}{2}\,\mathrm{tr}(\boldsymbol{s}^2) = \frac{1}{2}\left[\frac{E}{\alpha_2}\mathrm{tr}\,\boldsymbol{Y} + (\mathrm{tr}\boldsymbol{\sigma})^2\left(\frac{3\alpha_1\nu}{2\alpha_2} - \frac{1}{3}\right)\right]. \tag{43}$$

In a similar way the trace of the cubic power of the deviatoric stress tensor is

$$\mathrm{tr}(\boldsymbol{s}^3) = \mathrm{tr}(\boldsymbol{\sigma}^3) - I_1\,\mathrm{tr}(\boldsymbol{\sigma}^2) + \tfrac{2}{9}I_1^3. \tag{81}$$

Multiplying equation (51) with the stress tensor gives

$$\boldsymbol{\sigma}\,\boldsymbol{Y} = -\frac{\alpha_1\nu}{2E}(\mathrm{tr}\,\boldsymbol{\sigma})^2\boldsymbol{\sigma} + \frac{\alpha_2}{E}\boldsymbol{\sigma}^3, \tag{82}$$

which facilitates the expression for $\mathrm{tr}(\boldsymbol{\sigma}^3)$ in terms of $\mathrm{tr}(\boldsymbol{\sigma}\,\boldsymbol{Y})$ and $(\mathrm{tr}\,\boldsymbol{\sigma})^3$. Using then equation (81) results in expression (44):

$$\tilde{J}_3 = \frac{1}{3}\,\mathrm{tr}(\boldsymbol{s}^3) = \frac{1}{3}\left[\frac{E}{\alpha_2}(\mathrm{tr}(\boldsymbol{\sigma}\,\boldsymbol{Y}) - \mathrm{tr}\boldsymbol{\sigma}\mathrm{tr}\,\boldsymbol{Y}) + \left(\frac{2}{9} - \frac{\alpha_1\nu}{\alpha_2}\right)(\mathrm{tr}\boldsymbol{\sigma})^3\right]. \tag{44}$$

However, it should be noted that the expressions for the invariants $\tilde{J}_2$ and $\tilde{J}_3$ in terms of the invariants of the stress tensor $\boldsymbol{\sigma}$ and the thermodynamic force $\boldsymbol{Y}$ are not unique.

Acknowledgements

The authors would like to thank the anonymous reviewers for their careful reading of the manuscript and suggestions for improvements.

References

[1] C. Avram, I. Făcăoaru, I. Filimon, O. Mîrsu, and I. Tertea. *Concrete Strength and Strains*. Elsevier, 1981.

[2] M. Basista. Micromechanics of damage in brittle solids. In J.J. Skrzypek and A. Ganczarski, editors, *Anisotropic Behaviour of Damaged Materials*, volume 9 of *Lecture Notes in Applied and Computational Mechanics*, pages 221–258. Springer-Verlag, 2003.

[3] CEB-FIP. Model code 2010, volume 1. International Federation for Structural Concrete (fib), 2010. fib Bulletin 65.

[4] W.F. Chen. *Plasticity in Reinforced Concrete*. McGraw-Hill, 1982.

[5] K.B. Dahl. A failure criterion for normal and high strength concrete. Technical Report 286, Department of Structural Engineering, Technical University of Denmark, 1992.

[6] A. Dragon, D. Halm, and Th. Desoyer. Anisotropic damage in quasi-brittle solids: modelling, computational issues and applications. *Computer Methods in Applied Mechanics and Engineering*, 183(3-4):331–352, 2000. URL `http://dx.doi.org/10.1016/S0045-7825(99)00225-X`.

[7] M. Frémond. *Non-Smooth Thermomechanics*. Springer, Berlin, 2002.

[8] L.M. Kachanov. On the creep fracture time. *Iz. An SSSR Ofd. Techn. Nauk.*, (8): 26–31, 1958. (in Russian).

[9] D. Krajcinovic. Constitutive equations for damaging materials. *Journal of Applied Mechanics*, 50(2):355–360, 1983. doi: http://dx.doi.org/10.1115/1.3167044.

[10] D. Krajcinovic and G.U. Fonseka. The continuous damage theory of brittle materials–part i: general theory. *Journal of Applied Mechanics*, 48(2):809–815, 1981. doi: http://dx.doi.org/10.1115/1.3157739.

[11] H. Kupfer, H.K. Hilsdorf, and H. Rüsch. Behaviour of concrete under biaxial stresses. *Journal of the American Concrete Institute*, 66(8):656–666, 1969.

[12] J. Lee. *Theory and implementation of plastic-damage model for concrete structures under cyclic and dynamic loading*. PhD thesis, University of California, Berkeley, 1996.

[13] J. Lee and G.L. Fenves. Plastic-damage model for cyclic loading of concrete structures. *Journal of the Engineering Mechanics, ASCE*, 124(8):892–900, 1998. doi: http://dx.doi.org/10.1061/(ASCE)0733-9399(1998)124:8(892).

[14] J. Lubliner, J. Oliver, S. Oller, and E. Oñate. A plastic-damage model for concrete. *International Journal of Solids and Structures*, 25(3):299–326, 1989. doi: http://dx.doi.org/10.1016/0020-7683(89)90050-4.

[15] J. Mazars and G. Pijaudier-Cabot. From damage to fracture mechanics and conversely: a combined approach. *International Journal of Solids and Structures*, 33 (20-22):3327–3342, 1996. doi: http://dx.doi.org/10.1016/0020-7683(96)00015-7.

[16] M. Mikkola and P. Piila. Nonlinear response of concrete by use of the damage theory. In *Proceedings of the International Conference on Computer-Aided Analysis and design of Concrete Structures*, pages 179–189, Swansea, 1984. Pineridge Press.

[17] H. Müller et al. Constitutive modelling for high strength/high performance concrete. International Federation for Structural Concrete (fib), January 2008. fib Bulletin 42.

[18] S. Murakami and K. Kamiya. Constitutive and damage evolution equations of elastic-brittle materials based on irreversible thermodynamics. *International Journal of Mechanical Sciences*, 39(4):473–486, 1997. doi: http://dx.doi.org/10.1016/S0020-7403(97)87627-8.

[19] S. Nemat-Nasser and M. Hori. *Micromechanics: Overall Properties of Heterogeneous Materials*, volume 37 of *North-Holland series in Applied Mathematics and Mechanics*. North-Holland, 1993.

[20] N.S. Ottosen. A failure criterion for concrete. *Journal of the Engineering Mechanics, ASCE*, 103(EM4):527–535, August 1977.

[21] N.S. Ottosen. Nonlinear finite element analysis of concrete structures. Technical Report Risø-R-411, RisøNational Laboratory, DK-4000 Roskilde, Denmark, May 1980.

[22] N.S. Ottosen and M. Ristinmaa. *The Mechanics of Constitutive Modeling*. Elsevier, 2005.

[23] K. Willam and E.P. Warnke. Constitutive model for the triaxial behaviour of concrete. In *IABSE Proceedings*, volume 19, pages 1–30, 1975. Seminar on Concrete Structures Subjected to Triaxial Stresses, Bergamo, Italy May 17-19, 1974.

Saba Tahaei Yaghoubi and Juha Hartikainen
Aalto University
Department of Civil and Structural Engineering
P.O. Box 12100, FI-00076 Aalto, Finland
saba.tahaei@aalto.fi, juha.hartikainen@aalto.fi

Reijo Kouhia
Tampere University of Technology
Department of Mechanical Engineering and Industrial Systems
P.O. Box 589, FI-33101 Tampere, Finland
reijo.kouhia@tut.fi

Kari Kolari
VTT Technical Research Centre of Finland
P.O. Box 1806, FI-02044 VTT, Finland
Kari.Kolari@vtt.fi